Title: B cell-mediated maintenance of CD169^{+} cells is critical for liver regeneration

Kristina Behnke[1*], Yuan Zhuang[1*], Haifeng C. Xu[1], Balamurugan Sundaram[1], Maria Reich[2], Prashant V. Shinde[1], Jun Huang[1], Nastaran Fazel Modares[4], Alexei V. Tumanov[3], Robin Polz[4], Jürgen Scheller[4], Carl F. Ware[5], Klaus Pfeffer[6], Verena Keitel[2], Dieter Häussinger[2], Aleksandra A. Pandyra[2], Karl S. Lang[7+], and Philipp A. Lang[1+, #]

[1]Department of Molecular Medicine II, Medical Faculty, Heinrich Heine University, Universitätsstr. 1, 40225 Düsseldorf, Germany, [2]Department of Gastroenterology, Hepatology, and Infectious Diseases, Heinrich-Heine-University Düsseldorf, Universitätsstr. 1, 40225 Düsseldorf, Germany, [3]Department of Microbiology, Immunology & Molecular Genetics, University of Texas Health Science Center, San Antonio, TX 78229, [4]Institute of Biochemistry and Molecular Biology II, Medical Faculty, Heinrich Heine University, 40225 Düsseldorf, Germany, [5]Infectious and Inflammatory Diseases Research Center, Sanford Burnham Prebys Medical Discovery Research Institute, La Jolla, CA 92037, [6]Institute of Medical Microbiology and Hospital Hygiene, University Hospital, Heinrich-Heine-University, Düsseldorf, Germany, [7]Institute of Immunology, Medical Faculty, University of Duisburg-Essen, Hufelandstr. 55, Essen 45147, Germany.

Key words: partial hepatectomy, liver regeneration, B cells, lymphotoxin beta

* contributed equally to this work.

+ contributed equally to this work.

#Address correspondence to Philipp A Lang, M.D., Ph.D.

Department of Molecular Medicine II, Medical Faculty, Heinrich Heine University, Universitätsstr.1, 40225 Düsseldorf, Germany.

Tel: +49 2118113580

Email: langp@uni-duesseldorf.de

Abbreviations: ALT: alanine amino transferase; AST: aspartate amino transferase; DT: diphtheria toxin; DTR: diphtheria toxin receptor; CD169-DTR-DT: DT treated CD169-DTR; EGF: epidermal growth factor; HE: Hematoxylin and eosin stain; IL6: Interleukin 6; Lt: lymphotoxin; PCNA: proliferating cell nuclear antigen; PHx: partial hepatectomy; phospho-H3: phospho-Histone H3; S: splenectomy; Stat3: Signal transducer and activator of transcription 3; TGFβ: Transforming growth factor beta; TNFα: Tumor necrosis factor alpha; TUNEL: Terminal deoxynucleotidyl transferase (TdT) dUTP Nick-End Labeling; WT: wild type.

This study was supported by the German Research Council (SFB974, KFO217, LA-2558/5-1). Furthermore, this study was supported by the Jürgen Manchot Graduate School MOI III.

Abstract

The liver has an extraordinary capacity to regenerate via activation of key molecular pathways. However, central regulators controlling liver regeneration remain insufficiently studied. Here we show that B cell-deficient animals failed to induce sufficient liver regeneration after partial hepatectomy (PHx). Consistently, adoptive transfer of B cells could rescue defective liver regeneration. B cell mediated lymphotoxin beta production promoted recovery from PHx. Absence of B cells coincided with loss of splenic $CD169^+$ macrophages. Moreover, depletion of $CD169^+$ cells resulted in defective liver regeneration and decreased survival, which was associated with reduced hepatocyte proliferation. Mechanistically, $CD169^+$ cells contributed to liver regeneration by inducing hepatic IL-6 production and STAT3 activation. Accordingly, treatment of $CD169^+$ cell depleted animals with IL-6/Il-6R rescued liver regeneration and severe pathology following PHx. In conclusion, we identified $CD169^+$ cells to be a central trigger for liver regeneration, by inducing key signaling pathways important for liver regeneration.

Introduction

Liver disease is a global health problem with millions of patients worldwide suffering from infections, toxic liver damage and hepatocellular carcinoma. Liver tissue has an extraordinary potential to regenerate, an effect already described in greek mythology. Since then, several key molecular pathways have been discovered to play important roles during liver regeneration, including NF-κB, STAT3, and Erk(1). Following 70% reduction of liver mass through partial hepatectomy (PHx) tumor necrosis factor (TNF) is rapidly produced and TNF receptor 1 (TNFR1) signaling is required to induce liver regeneration(2). Furthermore, the TNF superfamily members lymphotoxin alpha and lymphotoxin (Lt) beta play a critical role during liver regeneration(3, 4). Consistently, mice deficient for both, TNFRp55 and Ltβ receptor show delayed hepatocyte proliferation, and impaired survival following PHx(5). Furthermore, a markedly increase in IL-6 concentrations in the serum can be detected following loss of liver mass, and IL-6 deficient mice show delayed liver regeneration following PHx(6-8). Consistently, treatment with combined IL-6 and soluble IL6 receptor can improve liver regeneration and induce rapid hepatocyte proliferation(6, 9). Moreover, epidermal growth factor (EGF) receptor ligands including TGF-α and amphiregulin are able to induce hepatocyte proliferation *in vitro*(1, 10). However, TGF-α deficient animals exhibit normal recovery following PHx(11). In turn, amphiregulin deficient animals show delayed proliferation following loss of liver mass(12). Consistently, specific deletion of EGFR in hepatocytes resulted into decreased liver regeneration following PHx(13). Notably, TNF levels were strikingly increased in $EGFR^{\Delta HEP}$ animals following PHx, suggesting that factors important for liver regeneration can compensate for each other(13). Central key players during liver regeneration however, remain still insufficiently studied.

The spleen is tightly connected to the liver with important blood circuits. Receiving its blood from the splenic artery, it feeds via the splenic vein after joining of the arteria mesenteria inferior and superior into the portal vein. Hence, cytokines and chemokines produced in the spleen can act directly on the liver. The spleen itself is organized in the red and white pulp, with the separating marginal zone including the marginal sinus in between (14, 15). B cells account for about 50% of all cells in the spleen and are located in the white pulp and the marginal zone(14). B cells are critical for organization of the lymphoid tissue, as B cell-deficient mice exhibit reduced presence of metallophilic CD169$^+$ macrophages (16). CD169$^+$ cells are located along the marginal sinus and ideally situated to capture pathogens(14, 17). Interestingly, maintenance of CD169$^+$ cells depend on Ltα and Ltβ(18-20). Specifically, B- and T-cell- specific Ltβ deficient mice, exhibit reduction of CD169$^+$ cells in the spleen (18, 19). Moreover, as spleen resident macrophages, CD169$^+$ cells can contribute to cytokine production during inflammation and infection(21-23). However, the contributions of B cells and CD169$^+$ cells during liver regeneration remain insufficiently characterized.

In this study, we identified B cells and CD169$^+$ cells as important players for liver regeneration following PHx. Specifically, genetic B cell deficiency resulted in reduced signaling cascades required for hepatocyte proliferation and limited survival following PHx. B cell-deficient mice exhibited reduced presence of CD169$^+$ cells, which were critical for liver regeneration. Depletion of CD169$^+$ cells resulted in reduced IL-6 expression and reduced regeneration following PHx. Consistently, treatment of CD169$^+$ cell depleted animals with IL-6/IL-6R could rescue the severe pathology we observed in our setting.

Materials and Methods:

Animals: This study was carried out in accordance with the German Animal Welfare Act and the guidelines of the Shoochow University. The protocol was approved by the local authorities. *Baffr*$^{-/-}$, *Jh*$^{-/-}$, *CD169-DTR* mice were described previously and were kept on a C57Bl/6 background(18, 24, 25). Laparotomy was performed predominantly on male mice at 10-14 weeks of age using isoflurane inhalation narcosis as previously described(26). For PHx the left lateral and the left and right median liver lobes together with the gall bladder were excised subsequent to a one-step ligature using a 5-0 silk suture tie (Ethicon, Somerville, NJ) (5). Sham operations were performed in an identical manner without ligating and removing liver lobes. For splenectomy, the splenic artery and vein was ligated with a single knot 5-0 silk suture at the same time as PHx or otherwise indicated in figure legend. Next, connective tissue and spleen was removed. Abdomen and peritoneum was closed with a running 5-0 PDS suture (Ethicon), and the skin with a running 6-0 nylon suture (Ethicon)(26). Directly after surgery and 24 and 48 h post PHx mice received 5 mg/kg Carprofen (Rimadyl, Pfizer, Würselen, Germany). As expected, splenectomized animals did not show any sign of pathology (Fig 1A). Mice exhibiting severe disease symptoms where sacrificed and considered as dead. CD169^{+} cells in the *CD169-DTR* animals were depleted by injecting 2 doses of 100ng diphtheria toxin (DT) (Sigma) before the partial hepatectomy (PHx). Wild-type (WT; C57Bl/6) mice were used as controls. Mice were 10-14 weeks old. For blood and tissue collection mice were anesthetized (100 mg/kg Ketamin, 10 mg/kg Xylazine; Vétoquinol GmbH, Ravensburg, Germany), weighed, and bled via the vena cava inferior and serum was collected. The liver and spleen were removed, rinsed in PBS and weighed to calculate the LW/BW ratio and the spleen weight. Liver and spleen samples were stored at -80 °C for Histology, RNA and protein extraction.

LtβR antibody treatment and IL-6/IL-6R injection: In order to induce LtβR signalling, mice were intraperitoneally injected with 2 doses of 200µg an agonist LtβR antibody (clone 4H8) 24h before and 24h after PHx (27). DT treated CD169-DTR mice were injected with 2 doses of 20µg IL-6/IL-6R protein 24h before and immediately after PHx.

Purification of B cells: For B cell purification, single-cell suspensions of splenocytes were enriched following the manufacturer's instructions with a CD45R (B220) MicroBeads mouse kit (Miltenyi).

Histology: Histological analysis on snap frozen tissue (liver, spleen) was performed and stained for hematoxylin/eosin (Sigma-Aldrich, St. Louis, MO, USA) and TUNEL (Terminal deoxynucleotidyl transferase (TdT) dUTP Nick-End Labeling) (Roche). Snap-frozen tissue sections were stained with a CD169 antibody (clone: MOMA-1, ABD Serotec), B220(eBioscience), Ki-67 (abcam), phospho-Histone H3 (Millipore).

Flow cytometry analysis: Different immune populations were identified in single cell solutions from naïve liver and spleen samples and spleen and liver samples newly regenerated (New), remaining lobes (Old)) 24, 48 hours after PHx using anti-B220, anti-CD21, anti-CD23, anti-PD-L1, anti-NK1.1, anti-CD3, anti-CD19, anti-CD11b, anti-Siglec-H, anti-CD8a and anti-CD11c antibodies, anti-major histocompatibility complex class II (MHC-II), anti-CD40, anti-CD80, anti-CD86, anti-F4/80, anti-Ly6C, anti-CD138, anti-IgM, anti-CD38, anti-CD62L, anti-CD5, anti-IgD, anti-CD1d antibodies and 7AAD. All antibodies were obtained from eBioscience (San Diego, CA), except anti-CD169 (3D6.112), which was obtained from AbD Serotec (Dusseldorf, Germany). For quantification of cell population, calibration beads were added to assess cell

numbers (BD, San Diego, CA).

Serum biochemistry:

Aspartate aminotransferase (AST, GOT) and alanine aminotransferase (ALT, GPT) were measured using the automated biochemical analyser Spotchem EZ SP-4430 (Arkray, Amstelveen, Netherlands) and the Spotchem EZ Reagent Strips Liver-1.

Quantitative RT-PCR: RNA purification and RT-PCR analyses of liver and spleen were performed according to the manufacturer's instructions (TRIzol reagent and iTaq^{TM} Universal probes or SYBR Green One-Step Kit, BioRad). Expression of *Ltα, Ltβ, IL-6, TNFα* was determined with FAM probes (Applied Biosystems). Expression levels of other genes were tested using the following primer sequences: Egf_F: AGAAGGCTACGAAGGAGACG; Egf_R: AGAGTCAGGGCAACTCAGTC; Hbegf_F:GCAAATGCCTCCCTGGTTAC;Hbegf_F:GGACGACAGTACTACAGCCA; Areg_F:GCGAGGATGACAAGGACCTA; Areg_R:TCGTTTCCAAAGGTGCACTG; Tgfa_F:GCTCTGGAGAACAGCACATC; Tgfa_R:ACATGCTGGCTTCTCTTCCT; Tgfb1_F:TTGCTTCAGCTCCACAGAGA;Tgfb1_R:CAGAAGTTGGCATGGTAGCC; Hgf_F: CCAGAGGTACGCTACGAAGT; Hgf_R: CTGTGTGATCCATGGGACCT; Fgf1_F: CTCGCAGACACCAAATGAGG; Fgf1_R: CTTCTTGAGGCCCACAAACC; Vegfa_F:TTGAGACCCTGGTGGACATC;Vegfa_R:GGGCTTCATCGTTACAGCAG; Vegfb_F:GCCACCAGAAGAAAGTGGTG;Vegfb_R:ATTGCCCATGAGTTCCATGC ;Vegfc_F:AGGCAGCTAACAAGACATGTCCAAC;Vegfc_R:GGGTCCACAGACAT CATGGAATC;Fgf2_F:GGACGGCTGCTGGCTTCTAA;Fgf2_R:CCAGTTCGTTTCA GTGCCACATAC;Pdgfb_F:ATGAAATGCTGAGCGACCAC;Pdgfb_R:TCCCTCGAG ATGAGCTTTCC; For analysis, the expression levels of all target genes were normalized to the β-actin expression or GAPDH (ΔCt). Gene expression values were calculated with the ΔΔCt method, with untreated WT mice as controls to which all other

samples were normalized. Relative quantities (RQ) were determined with the equation RQ = 2^-ΔΔCt.

Immunoblotting: Liver tissue was lysed in PBS containing 1% Triton X-100, Protease inhibitors (Sigma), PhosSTOP (1 tablet/10 ml). Immunoblots were probed with primary antibody: Phospho-Stat3, Stat3, Phospho-Erk1/2, Erk1/2, IκBα, IL-6, PCNA and β-actin (Cell Signalling technology), followed by secondary antibody and chemiluminescence (ECL) detection or Florence secondary antibody and detected by LICOR.

Statistical analyses: Data are expressed as mean ± S.E.M. Statistical significant differences between two different groups were analysed using student's t test. Statistically significant differences between groups in experiments involving more than one time-point were determined with two-way ANOVA (repeated measurements). All the quantifications were analysed by ImageJ.

Results

B cells are important for liver regeneration.

Based on previous data describing a beneficial role of the spleen during liver regeneration following partial hepatectomy (PHx) in mice(28), we found that a proportion of splenectomized C57Bl/6 mice developed severe pathology (Fig. 1A+Suppl. Fig. 1A). Consistently, liver weight/body weight ratio following PHx was reduced in absence of spleen tissue when compared to PHx controls (Fig. 1B)(28). Moreover, alanine aminotransferase (ALT) and aspartate aminotransferase (AST) activity, indicators of liver damage were markedly increased in the blood of splenectomized mice after PHx compared to PHx only or splenectomy controls (Suppl. Fig. 1B). Although splenectomized mice exhibited histological changes in liver tissue, we did not observe a significant increase in TUNEL staining (Suppl. Fig. 1C+D). However, staining for proliferation indicators such as Ki-67 and Phospho-Histone H3 (Phospho-H3) was reduced in liver tissue of splenectomized animals (Fig. 1C+D+Suppl. Fig. 1E). Next, we investigated, which splenic factors may be important for liver regeneration. B cells account for about 50% of all cells in the spleen and are located in the white pulp and the marginal zone (14). However, we did not observe any difference in the presence of B cell subsets following PHx surgery in the spleen and liver (Fig. 1E+Suppl. Fig. 2A-C), while T cell numbers increased in the regenerating liver tissue following PHx, which is consistent with the literature (Suppl. Fig. 2D)(4). Nevertheless, when we subjected B cell deficient *Jh*$^{-/-}$ mice to PHx, we found reduced survival following PHx when compared to WT controls (Fig. 1F). This effect was not due to surgery complications or infection, as Sham-operated *Jh*$^{-/-}$ mice showed no signs of disease and survived after surgery (Fig. 1F). In contrast to splenectomized mice, B cell-deficient animals did not exhibit increased activity of liver transaminases when

compared to WT controls (Fig. 2A). Consistently, we could not detect histological differences or increased TUNEL staining following PHx in *Jh*$^{-/-}$ mice compared to WT mice (Fig. 2B + Suppl. Fig. 3A). Deficiency of the B cell survival promoting B cell activating factor of the TNF family (BAFF) results in B cell lymphopenia in mice and man (25, 29). Accordingly, *Baffr*$^{-/-}$ mice displayed severe disease symptoms following PHx compared to WT and Sham-operated mice (Fig. 2C). In parallel to *Jh*$^{-/-}$ mice, *Baffr*$^{-/-}$ animals exhibited only slight increase in liver transaminases and to control liver tissue comparable histological appearance in H&E tissue sections (Fig. 2D + Suppl. Fig. 3B). However, expression of Phospho-Histone H3 (Phospho-H3) was reduced in B cell-deficient and BAFFR deficient mice compared to WT controls following PHx (Fig. 2E + Suppl. Fig. 3C+D). Furthermore, expression of Ki-67 was delayed in absence of B cells or BAFFR (Figure. 2F+ Suppl. Fig. 3E+F). These data indicate that B cells provide important factors for hepatocyte proliferation and liver regeneration. Next, we wondered, which B cell derived factors are important for liver regeneration. B cells express Ltα and Ltβ, which are critical for lymphoid tissue organization. We found decreased expression level of *Ltβ* in *Jh*$^{-/-}$ mice compared to WT controls both in the spleen and liver after PHx and also naïve mice (Fig. 3A+B), while the difference in Ltα expression was not significant after PHx in the liver in our setting (Suppl. Fig. 4). This opted us to speculate that Ltβ plays a major role in regulating B cell-mediated liver regeneration in our settings. To further validate that Ltβ is produced by B cells, we adoptively transferred B cells into *Jh*$^{-/-}$ mice (Fig. 3C), which rescued Ltβ expression levels in the liver (Fig. 3D+E). Consistently, when we adoptively transferred B cells into *Jh*$^{-/-}$ mice, we could rescue severe disease development following PHx (Fig. 3F). Furthermore, B cell transfer into partially hepatectomized *Baffr*$^{-/-}$ mice prevented severe disease (Fig. 3G). Since lymphtoxins are known to be critical for liver regeneration(30),

we hypothesized that B cell-derived-Ltβ expression may contribute to liver regeneration. Consistently, when we applied an agonistic anti-LtβR antibody prior to PHx, we observed protection of *Jh*$^{-/-}$ mice (Fig. 3H). Taken together, these data indicate that B cells are critical to contribute towards liver regeneration.

CD169^{+} cells are critical for liver regeneration following PHx.

Ltα and Ltβ are important cytokines for the maintenance of CD169^{+} macrophages in the spleen(18-20). B cells are critical for organization of the lymphoid tissue, as B cell-deficient mice exhibit reduced presence of metallophilic CD169^{+} macrophages (Fig. 4A+ B) (15, 23). Following adoptive transfer of B cells into *Jh*$^{-/-}$ mice CD169^{+} cells were restored (Fig. 4C). Therefore, we hypothesized that B cell-mediated maintenance of CD169^{+} cells contribute to liver regeneration. Interestingly, we observed higher numbers of CD169^{+} cells in the regenerating, but also the remaining liver lobe using flow cytometry (Fig. 4D). Notably, following splenectomy the increase of CD169^{+} cells was abolished (Suppl. Fig. 5A). Furthermore, we observed a slight increase of CD169^{+} cells in the spleen compared to unoperated mice (Fig. 4E). CD169^{+} cells can be depleted by injection of diphtheria toxin into CD169-DTR mice (24). To exclude effects of DT on other cell types, we administered DT to WT mice before and after PHx and observed no effects in liver regeneration and survival (Suppl. Fig. 5B+C). Absence of CD169^{+} cells resulted in slightly increased AST activity in the serum after PHx when compared to WT controls (Fig. 4F). Furthermore, DT-treated CD169-DTR mice succumbed after PHx compared to control mice (Fig. 4G). Taken together, we identified CD169^{+} cells to be important for liver regeneration following PHx.

Consistent with the findings in B cell-deficient mice, we observed no histological differences in absence or presence of CD169^{+} cells in H&E tissue sections (Suppl. Fig.

5D). Moreover, we could not detect increased TUNEL staining following PHx in DT-treated CD169-DTR mice compared to untreated controls (Suppl. Fig. 5E). However, we observed delayed liver regeneration following PHx in DT-treated CD169-DTR mice in comparison to control animals as evident by decreased liver/body weight ratio (Fig. 5A). Furthermore, we found reduced presence of phospho-H3 and reduced expression of Ki-67 cells in the liver tissue in DT-treated CD169-DTR mice in comparison to control animals (Fig. 5B+C + Suppl. Fig. 5F). Consistently, expression of proliferating cell nuclear antigen (PCNA), which is involved in DNA repair and synthesis was reduced in the liver as a result of $CD169^+$ cell depletion compared to WT mice following PHx (Fig. 5D). We next analyzed the liver morphology in DT-treated CD169-DTR mice at later time points such as 13 days after PHx. We observed a slight, but significant reduction in liver weight in DT-treated mice compared to untreated controls (Fig. 5E). Together these data suggest that $CD169^+$ cells promote proliferation following PHx and therefore contribute to liver regeneration.

$CD169^+$ cells promote IL-6 production during liver regeneration

To define how $CD169^+$ cells contribute to liver regeneration we analyzed RNA expression levels of genes encoding for cytokines important for liver regeneration (Fig. 6A). We found decreased IL-6 expression in B cell-deficient mice in the liver when compared to control animals in our setting (Figure. 6A+B). Transfer of B cells into $Jh^{-/-}$ mice could restore *IL-6* expression levels in the liver (Fig. 6C). IL-6-deficient mice show delayed liver regeneration (6-8). We speculated that $CD169^+$ cells might trigger liver regeneration by inducing expression of IL-6. In line with that, DT-treated CD169-DTR mice showed reduced RNA expression levels of *Il-6* in liver tissue compared to control animals 6 and 48 hours after PHx (Fig. 6D+E). Moreover, IL-6 expression was

reduced on a protein level 48 hours following PHx in absence of CD169$^+$ cells (Fig. 6F). Notably, we also observed early increase in *Il-6* expression levels in absence of CD169$^+$ cells, and accordingly STAT3 phosphorylation 12 hours after PHx (Fig. 6D+G). However, consistent with the reduced expression of IL-6, we observed lower expression of phospho-STAT3 in liver tissue harvested from CD169$^+$ cell deficient mice compared to CD169$^+$ cell competent mice 24 and 48 hours after PHx (Fig. 6G + Suppl. Fig. 6). Notably, we observed similar induction of phospho-Erk and similar decrease of IκBα, indicating that other signaling pathways participating in liver regeneration remain intact in the absence of CD169$^+$ cells in our settings (Fig. 6G + Suppl. Fig. 6).

To explore whether IL-6R signaling can compensate for CD169$^+$ cells, we administered IL-6/IL-6R protein before and after PHx in DT treated CD169-DTR (6). As expected, we found increased STAT3 phosphorylation following injection with IL-6/IL-6R in both, CD169$^+$ cell competent or depleted animals (Fig. 7A). Notably, liver weight/body weight ratio in CD169-DTR DT treated animals after PHx following treatment with IL-6/IL-6R was comparable to untreated CD169-DTR mice following PHx (Fig. 7B), indicating that injection of IL-6/IL-6R could restore liver regeneration in CD169$^+$ cell depleted mice. Consistently, we found increased expression of phosphor-H3 and Ki-67 following treatment with IL-6/IL-6R of CD169-DTR mice when compared to CD169-DTR controls (Fig. 7C). Moreover, PCNA expression was increased after IL-6/IL-6R treatment in absence of CD169$^+$ cells after PHx (Fig. 7D). Furthermore, we found that IL-6/IL-6R protein significantly rescued the pathology following PHx in CD169-DTR animals (Fig. 7E). In conclusion, we identified that B cell-mediated maintenance of CD169$^+$ cells contributes to IL-6 production and liver regeneration.

Discussion

In this study, we identify that B cells promoted maintenance of $CD169^+$ cells, which are critical for liver regeneration. Consistently, depletion of $CD169^+$ cells resulted in reduced IL-6 expression following PHx and consequently reduced activation of STAT3 signaling pathways. Application of IL-6/IL-6R could rescue defective liver regeneration in absence of $CD169^+$ cells.

Liver regeneration is triggered by key signaling pathways, which are regulated through several cytokines. Specifically, the TNF superfamily members TNF, Ltα, and Ltβ have been shown to be important for liver regeneration. Ltα and Ltβ production by T cells play an important role during liver regeneration. Notably, B- and T-cell -specific LTα and LTβ deficient mice display also reduced presence of $CD169^+$ cells(19). Hence, lymphotoxin could not only exhibit effects on hepatocytes, but also on $CD169^+$ cells and thereby affect IL-6-mediated signaling. Specifically, we observed reduced IL-6 expression in liver tissue from DT-treated CD169-DTR mice compared to control animals. Consistently, defective IL-6 signaling results into impaired liver regeneration, a transient effect, which can result in altering severity of the phenotype (6, 7). Similarly, we observed severe pathology in a proportion of animals following splenectomy and PHx albeit other studies, which also reported a supporting role of the spleen during liver regeneration in mice, did not indicate a severe pathology (28). Since at later time points we observed only slight, but significant decrease in liver mass in absence of $CD169^+$ cells, the effects described here might be also transient. We speculated that underlying mechanisms following defective liver regeneration in B cell and $CD169^+$ cell deficient animals likely preceded the development of disease symptoms and therefore analyzed early time points following PHx. Consistently, we found reduced presence of proliferation markers and reduced liver weight/body weight ratio during these time points. However, treatment with IL-6/IL-6R improved expression of hepatic

proliferation markers, liver weight/body weight ratio, and observed pathology in absence of $CD169^+$ cells (6).

The spleen is ideally situated to trigger liver regeneration. The blood from spleen tissue directly feeds into the portal vein circulation. Accordingly, cytokines and chemokines produced in the spleen are able to trigger their effects in the liver. As discussed above, several immune factors contribute to or regulate liver regeneration. Splenectomy has been shown to be beneficial in clinical settings of liver cirrhosis and portal hypertension or hypersplenism(31, 32). These beneficial effects have been attributed towards reduction of the portal circulation(33). Furthermore, experiments using rats have shown, that splenectomy can result in reduced concentrations of TGFβ, and consequently reduced inhibitory effects on liver regeneration(34, 35). Interestingly, these effects increase with the amount of liver mass removed(35). In mice, splenectomy results in delayed liver regeneration following PHx(28). The role of B cells in the regulation of liver functions during the acute and chronic liver disease remains controversial (36, 37). In our settings, splenectomy, B cell deficiency, and deletion of $CD169^+$ cells resulted in impaired liver regeneration following PHx. One explanation could be that in rats $CD169^+$ cells from other lymphoid tissue compensate for loss of splenic $CD169^+$ cells. Furthermore, increased IL-6/IL-6R signaling might compensate for the splenic loss of $CD169^+$ cells. In our setting, treatment with IL-6/IL-6R could prevent severe pathology in absence of $CD169^+$ cells. Future studies could compare the activation of B cells and $CD169^+$ cells during chronic liver disease and liver pathology.

In conclusion, we identified in our model systems, that B cell-mediated maintenance of $CD169^+$ cells contributes to liver regeneration.

References:

1. Michalopoulos GK. Liver regeneration after partial hepatectomy: critical analysis of mechanistic dilemmas. Am J Pathol 2010;176:2-13.

2. Yamada Y, Kirillova I, Peschon JJ, Fausto N. Initiation of liver growth by tumor necrosis factor: Deficient liver regeneration in mice lacking type I tumor necrosis factor receptor. Proceedings of the National Academy of Sciences of the United States of America 1997;94:1441-1446.

3. Anders RA, Subudhi SK, Wang J, Pfeffer K, Fu YX. Contribution of the lymphotoxin beta receptor to liver regeneration. J Immunol 2005;175:1295-1300.

4. Tumanov AV, Koroleva EP, Christiansen PA, Khan MA, Ruddy MJ, Burnette B, Papa S, et al. T Cell-Derived Lymphotoxin Regulates Liver Regeneration. Gastroenterology 2009;136:694-704.

5. Sorg UR, Behnke K, Degrandi D, Reich M, Keitel V, Herebian D, Deenen R, et al. Cooperative role of lymphotoxin beta receptor and tumor necrosis factor receptor p55 in murine liver regeneration. J Hepatol 2015.

6. Schmidt-Arras D, Rose-John S. IL-6 pathway in the liver: From physiopathology to therapy. Journal of Hepatology 2016;64:1403-1415.

7. Cressman DE, Greenbaum LE, DeAngelis RA, Ciliberto G, Furth EE, Poli V, Taub R. Liver failure and defective hepatocyte regeneration in interleukin-6-deficient mice. Science 1996;274:1379-1383.

8. Sakamoto T, Liu Z, Murase N, Ezure T, Yokomuro S, Poli V, Demetris AJ. Mitosis and apoptosis in the liver of interleukin-6-deficient mice after partial hepatectomy. Hepatology 1999;29:403-411.

9. Peters M, Blinn G, Jostock T, Schirmacher P, Zum Buschenfelde KHM, Galle PR, Rose-John S. Combined interleukin 6 and soluble interleukin 6 receptor accelerates murine liver regeneration. Gastroenterology 2000;119:1663-1671.

10. Block GD, Locker J, Bowen WC, Petersen BE, Katyal S, Strom SC, Riley T, et al. Population expansion, clonal growth, and specific differentiation patterns in primary cultures of hepatocytes induced by HGF/SF, EGF and TGF alpha in a chemically defined (HGM) medium. Journal of Cell Biology 1996;132:1133-1149.

11. Russell WE, Kaufmann WK, Sitaric S, Luetteke NC, Lee DC. Liver regeneration and hepatocarcinogenesis in transforming growth factor-alpha-targeted mice. Molecular Carcinogenesis 1996;15:183-189.

12. Berasain C, Garcia-Trevijano ER, Castillo J, Erroba E, Lee DC, Prieto J, Avila MA. Amphiregulin: An early trigger of liver regeneration in mice. Gastroenterology 2005;128:424-432.

13. Natarajan A, Wagner B, Sibilia M. The EGF receptor is required for efficient liver regeneration. Proc Natl Acad Sci U S A 2007;104:17081-17086.

14. Junt T, Scandella E, Ludewig B. Form follows function: lymphoid tissue microarchitecture in antimicrobial immune defence. Nat Rev Immunol 2008;8:764-775.

15. Davies LC, Jenkins SJ, Allen JE, Taylor PR. Tissue-resident macrophages. Nature Immunology 2013;14:986-995.

16. Nolte MA, Arens R, Kraus M, van Oers MH, Kraal G, van Lier RA, Mebius RE. B cells are crucial for both development and maintenance of the splenic marginal zone. J Immunol 2004;172:3620-3627.

17. Honke N, Shaabani N, Cadeddu G, Sorg UR, Zhang DE, Trilling M, Klingel K, et al. Enforced viral replication activates adaptive immunity and is essential for the control of a cytopathic virus. Nat Immunol 2012;13:51-57.

18. Tumanov A, Kuprash D, Lagarkova M, Grivennikov S, Abe K, Shakhov A, Drutskaya L, et al. Distinct role of surface lymphotoxin expressed by B cells in the organization of secondary lymphoid tissues. Immunity 2002;17:239-250.

19. Tumanov AV, Grivennikov SI, Shakhov AN, Rybtsov SA, Koroleva EP, Takeda J, Nedospasov SA, et al. Dissecting the role of lymphotoxin in lymphoid organs by conditional targeting. Immunol Rev 2003;195:106-116.

20. Futterer A, Mink K, Luz A, Kosco-Vilbois MH, Pfeffer K. The lymphotoxin beta receptor controls organogenesis and affinity maturation in peripheral lymphoid tissues. Immunity 1998;9:59-70.

21. Asano K, Takahashi N, Ushiki M, Monya M, Aihara F, Kuboki E, Moriyama S, et al. Intestinal CD169(+) macrophages initiate mucosal inflammation by secreting CCL8 that recruits inflammatory monocytes. Nature Communications 2015;6.

22. Moseman EA, Iannacone M, Bosurgi L, Tonti E, Chevrier N, Tumanov A, Fu YX, et al. B cell maintenance of subcapsular sinus macrophages protects against a fatal viral infection independent of adaptive immunity. Immunity 2012;36:415-426.

23. Xu HC, Huang J, Khairnar V, Duhan V, Pandyra AA, Grusdat M, Shinde P, et al. BAFFR deficiency results in limited CD169+ macrophage function during viral infection. J Virol 2015.

24. Asano K, Nabeyama A, Miyake Y, Qiu CH, Kurita A, Tomura M, Kanagawa O, et al. CD169-positive macrophages dominate antitumor immunity by crosspresenting dead cell-associated antigens. Immunity 2011;34:85-95.

25. Sasaki Y, Casola S, Kutok JL, Rajewsky K, Schmidt-Supprian M. TNF family member B cell-activating factor (BAFF) receptor-dependent and -independent roles for BAFF in B cell physiology. J Immunol 2004;173:2245-2252.

26. Greene AK, Puder M. Partial hepatectomy in the mouse: technique and perioperative management. J Invest Surg 2003;16:99-102.

27. Dejardin E, Droin NM, Delhase M, Haas E, Cao Y, Makris C, Li ZW, et al. The lymphotoxin-beta receptor induces different patterns of gene expression via two NF-kappaB pathways. Immunity 2002;17:525-535.

28. Furuya S, Kono H, Hara M, Hirayama K, Tsuchiya M, Fujii H. Interleukin-17A plays a pivotal role after partial hepatectomy in mice. J Surg Res 2013;184:838-846.

29. Warnatz K, Salzer U, Rizzi M, Fischer B, Gutenberger S, Bohm J, Kienzler AK, et al. B-cell activating factor receptor deficiency is associated with an adult-onset antibody deficiency syndrome in humans. Proc Natl Acad Sci U S A 2009;106:13945-13950.

30. Tumanov AV, Koroleva EP, Christiansen PA, Khan MA, Ruddy MJ, Burnette B, Papa S, et al. T cell-derived lymphotoxin regulates liver regeneration. Gastroenterology 2009;136:694-704 e694.

31. Kawanaka H, Akahoshi T, Kinjo N, Harimoto N, Itoh S, Tsutsumi N, Matsumoto Y, et al. Laparoscopic Splenectomy with Technical Standardization and Selection Criteria for Standard or Hand-Assisted Approach in 390 Patients with Liver Cirrhosis and Portal Hypertension. Journal of the American College of Surgeons 2015;221:354-366.

32. Tomikawa M, Akahoshi T, Sugimachi K, Ikeda Y, Yoshida K, Tanabe Y, Kawanaka H, et al. Laparoscopic splenectomy may be a superior supportive intervention for cirrhotic patients with hypersplenism. Journal of Gastroenterology and Hepatology 2010;25:397-402.

33. Eipel C, Abshagen K, Ritter J, Cantre D, Menger MD, Vollmar B. Splenectomy improves survival by increasing arterial blood supply in a rat model of reduced-size liver. Transplant International 2010;23:998-1007.

34. Lee SC, Jeong HJ, Choi BJ, Kim SJ. Role of the spleen in liver regeneration in relation to transforming growth factor-beta 1 and hepatocyte growth factor. Journal of Surgical Research 2015;196:270-277.

35. Kim J, Kim CJ, Ko IG, Joo SH, Ahn HJ. Splenectomy affects the balance between hepatic growth factor and transforming growth factor-beta and its effect on liver regeneration is dependent on the amount of liver resection in rats. J Korean Surg Soc 2012;82:238-245.

36. Novobrantseva TI, Majeau GR, Amatucci A, Kogan S, Brenner I, Casola S, Shlomchik MJ, et al. Attenuated liver fibrosis in the absence of B cells. J Clin Invest 2005;115:3072-3082.

37. Richards JA, Bucsaiova M, Hesketh EE, Ventre C, Henderson NC, Simpson K, Bellamy CO, et al. Acute Liver Injury Is Independent of B Cells or Immunoglobulin M. PLoS One 2015;10:e0138688.

Figure Legends:

Figure 1: Decreased liver regeneration in splenectomized and B cell deficient mice following PHx. (A) Survival of splenectomized, 70 % PHx, and splenectomized mice followed by PHx (PHx+S) was monitored (n=14-19). **(B)** Liver weight/ body weight ratio was determined at indicated time points in WT sham operated mice and splenectomized mice (left panel), and PHx operated WT mice and splenectomized mice (PHx+S) (right panel) (n=3-5). **(C-D)** Sections of Snap-frozen liver tissue from 70 % PHx and splenectomized mice followed by PHx (PHx+S) at indicated time points were stained with **(C)** anti-phospho-H3 and **(D)** anti-Ki-67 antibodies. Representative sections for each time point are shown (n=4, scale bar=100μm). Right panels indicate quantification. **(E)** B cell numbers were determined by flow cytometry in the newly regenerated (New) (n=7-8), and remaining (Old) liver lobes(n=3-4) and spleen tissue (n=7-8) at indicated time points after 70% PHx. Results were calculated according to the liver (g) and spleen weight (mg). (**F**) Survival of *Jh*$^{-/-}$ mice (n=9) after 70% PHx compared to sham operated *Jh*$^{-/-}$ mice (n=3) and WT mice (n=6). Error bar in the all the above experiments represent SEM; **P* < 0.05, ***P* < 0.01, *** *P* < 0.001.

Figure 2: B cells play a crucial role for liver regeneration after PHx. (A) The activity of aspartate aminotransferase (AST) and alanine aminotransferase (ALT) was measured in serum of WT and *Jh*$^{-/-}$ mice following PHx at indicated time points (n=4-5). **(B)** Sections of Snap-frozen liver tissue from WT and *Jh*$^{-/-}$ mice following PHx were stained with H&E. One representative set of n=3 is shown. (Scale bar = 200μm). **(C)** Survival of *Baffr*$^{-/-}$ mice (n=18) after 70% PHx compared to sham operated *Baffr*$^{-/-}$ mice (n=4) and WT mice after 70% PHx was monitored (n=7). **(D)** The activity of aspartate aminotransferase (AST) and alanine aminotransferase (ALT) was measured in serum of

WT and *Baffr*$^{-/-}$ mice following PHx at indicated time points (n=4-5). **(E-F)** Sections of Snap-frozen liver tissue from WT and *Jh*$^{-/-}$ mice following PHx were stained with **(E)** anti-phospho-H3 and **(F)** anti-Ki-67 antibodies. Representative sections for each time point are shown (n=3, scale bar=100μm). Lower panels indicate quantification. Error bar in the all the above experiments represent SEM, *$P < 0.05$, **$P < 0.01$, *** $P < 0.001$.

Figure 3: B cell-derived lymphotoxin beta contributes to liver regeneration after PHx. (A) RNA expression of *Ltβ* was measured in spleen and liver tissue from WT and *Jh*$^{-/-}$ mice at the indicated time points post 70% PHx (n=3-4). **(B)** Protein level of Ltβ was measured in liver tissue from naïve WT and *Jh*$^{-/-}$, and WT and *Jh*$^{-/-}$ mice at the indicated time points post 70% PHx. **(C-E)** $2*10^6$ purified B cells from WT mice were intravenously injected into *Jh*$^{-/-}$ mice. After 48 hours, **(C)** B cell numbers were determined in the spleen by flow cytometry (n=4-6), **(D)** RNA levels of *Ltβ* were measured in liver tissue(n=3-5), and **(E)** Protein level of Ltβ was measured in liver tissue. **(F)** Survival of *Jh*$^{-/-}$ mice without (n=6) or after B cell transfer (n=7) was determined following 70% PHx. **(G)** Survival of *Baffr*$^{-/-}$ mice without (n=7) or after B cell transfer (n=7) was determined following 70% PHx. **(H)** Survival of untreated (n=13) and agonist LtβR antibody treated (n=13) *Jh*$^{-/-}$ mice was monitored after 70% PHx. Error bar in the all the above experiments represent SEM; *$P < 0.05$, **$P < 0.01$.

Figure 4: CD169$^+$ cells contribute to liver regeneration. (A) Sections of snap-frozen spleen tissue from WT and *Jh*$^{-/-}$ mice were stained with anti-CD169, anti-B220 and anti-CD90.2 antibodies. Representative sections are shown (n=4-5, scale bar=100μm). Right panel indicates average and SEM of mean fluorescence intensities (MFI) of CD169 stainings. **(B)** Sections from snap-frozen spleen tissue from WT and *Baffr*$^{-/-}$ mice were

stained with anti-CD169 anti-B220 and anti-CD90.2 antibodies. Representative sections are shown (n=4-5, scale bar=100μm). Right panel indicates average and SEM of mean fluorescence intensities (MFI) of CD169 stainings. **(C)** $2*10^6$ purified B cells from WT mice were adoptively transferred into *Jh*$^{-/-}$ mice. After 48 hours, CD169 cell numbers were determined in the spleen by flow cytometry (n=4-6). **(D-E)** CD169$^+$ cells were measured by flow cytometry in the newly regenerated (n=7-8) and remaining (Old) (n=3-4) liver lobes **(D)** and spleen tissue (n=7-8) **(E)** at the indicated time points after 70% PHx. Results were calculated according to the liver (g) and spleen weight (mg). **(F)** The activity of aspartate aminotransferase (AST) and alanine aminotransferase (ALT) was measured in serum of WT and DT treated CD169-DTR mice following PHx at indicated time points (n=3). **(G)** Survival of DT treated CD169-DTR mice after PHx (n=12) compared to WT mice (n=8) after PHx, CD169-DTR mice (n=5) after PHx and sham operated DT treated CD169-DTR mice (n=4) and was monitored. Error bar in the all the above experiments represent SEM; *$P < 0.05$, **$P < 0.01$, ****$P < 0.0001$.

Figure 5: CD169$^+$ cells promotes presence of hepatic proliferation markers after PHx. (A) Liver weight/ body weight ratio was determined after 70 % PHx in DT treated WT mice and DT-treated CD169-DTR mice followed by PHx (n=3). **(B-C)** Sections of snap-frozen liver tissue from CD169-DTR and DT-treated CD169-DTR mice at indicated time points after 70% PHx were stained with anti-Phospho-H3 **(B)** and anti-Ki-67 **(C)** antibodies. Representative sections for each time point are shown (n=3, scale bar= 100μm). Right panels indicate quantification. **(D)** Protein level of PCNA was measured at indicated time points after 70 % PHx in DT-treated CD169-DTR and CD169-DTR mice (n=4). Lower panel indicates quantification. **(E)** liver weight (left panel) and Liver morphology (g, right panel) was determined at day 13 after 70% PHx

of DT-treated CD169-DTR and CD169-DTR mice (n=3-5). Error bar in the all the above experiments represent SEM; *$P < 0.05$, **$P < 0.01$, ***$P < 0.001$

Figure 6: Defective activation of IL-6 signalling in absence of CD169$^+$ cells. (A) RNA expression level of cytokines important for liver regeneration was determined in the liver tissue from WT and *Jh*$^{-/-}$ mice at the indicated time points post 70% PHx (n=3). **(B)** Protein expression of IL-6 was determined in liver tissue from WT and *Jh*$^{-/-}$ mice at the indicated time points after 70% PHx (n=3). Lower panel indicates quantification. **(C)** RNA expression levels of *IL-6* was measured in the liver tissue of WT and *Jh*$^{-/-}$ mice without or with purified B cells (n=3-5). **(D-E)** RNA expression levels of *Il-6* were determined in liver tissue from DT treated WT, CD169-DTR and DT treated CD169 DTR mice as labelled at the indicated time points after 70% PHx (n=3-5). **(F)** Protein expression of IL-6 was determined in liver tissue from CD169-DTR and DT treated CD169-DTR mice at the indicated time points after 70% PHx (n=3). Lower panel indicates quantification. **(G)** Protein lysates of liver tissue from CD169-DTR mice and DT treated CD169-DTR mice at indicated time points after PHx were blotted and stained with anti-phospho-Erk, anti-Erk, anti-phospho-STAT3, anti-STAT3, anti-IκBα and anti-β-actin antibodies (one representative of n=3 blots is shown). Error bar in the all the above experiments represent SEM; *$P < 0.05$, **$P < 0.01$, ***$P < 0.001$.

Figure 7: IL-6/IL-6R treatment can rescue liver regeneration in absence of CD169$^+$ cells. (A) Protein lysates of liver tissue from CD169-DTR mice or DT treated CD169-DTR mice following IL-6/IL-6R treatment were blotted and stained with anti-phospho-Erk, anti-Erk, anti-phospho-STAT3, anti-STAT3, anti-IκBα and anti-β-actin antibodies.

One representative of n=6 blots is shown. Right panels indicate quantification. **(B)** Liver weight/body weight ratio was determined at 48 hours after 70 % PHx in CD169-DTR mice and DT-treated CD169-DTR mice and following IL-6/IL-6R treatment (n=3-5). **(C-D)** Sections of snap-frozen liver tissue from DT treated CD169-DTR mice without or after IL-6/IL-6R treatment at 48hours after 70% PHx were stained with **(C)** anti-Phospho-H3 and **(D)** anti-Ki-67 antibodies. Representative sections for each time point are shown (n=3-5, scale bar C=50µm, D=100µm). Right panels indicate quantification. **(E)** Protein level of PCNA was measured in DT treated CD169-DTR mice in absence and presence of IL-6/IL-6R treatment at 48 hours after 70% PHx (n=5). Lower panel indicates quantification. **(F)** Survival of DT treated CD169-DTR mice without or after IL-6/IL-6R treatment was monitored (n=8-9). Error bar in the all the above experiments represent SEM; $*P < 0.05$, $**P < 0.01$, $***P < 0.001$.

Figure 1

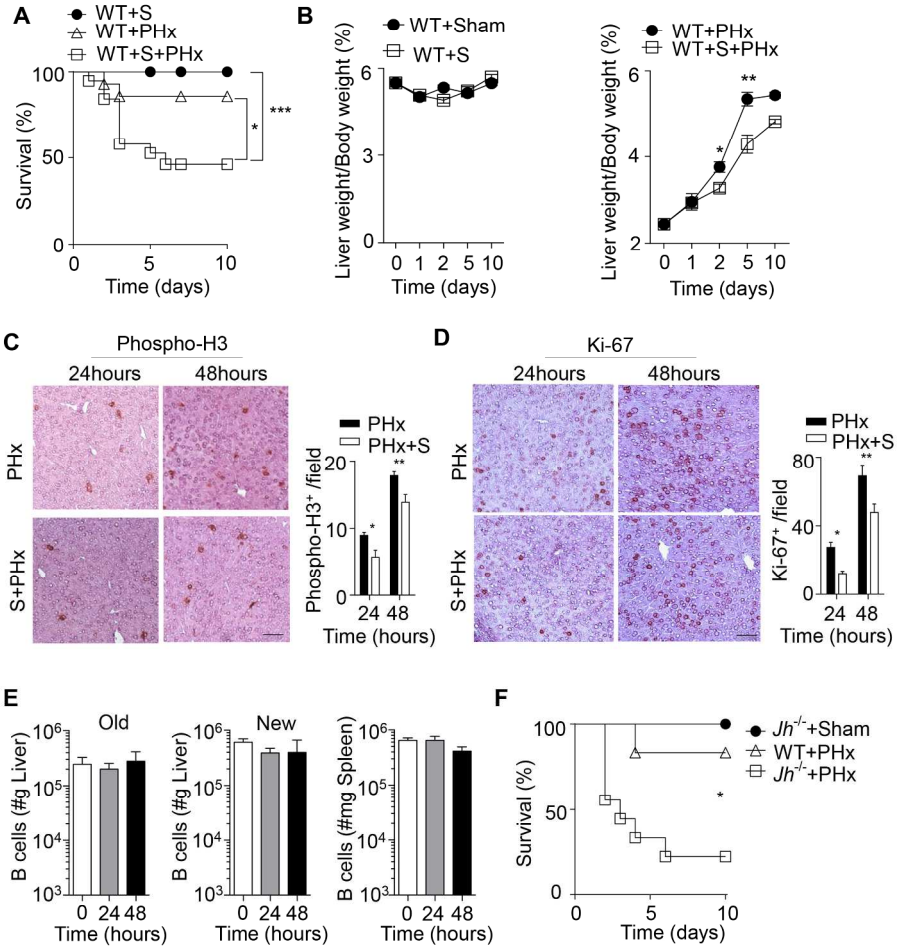

190x254mm (300 x 300 DPI)

Figure 2

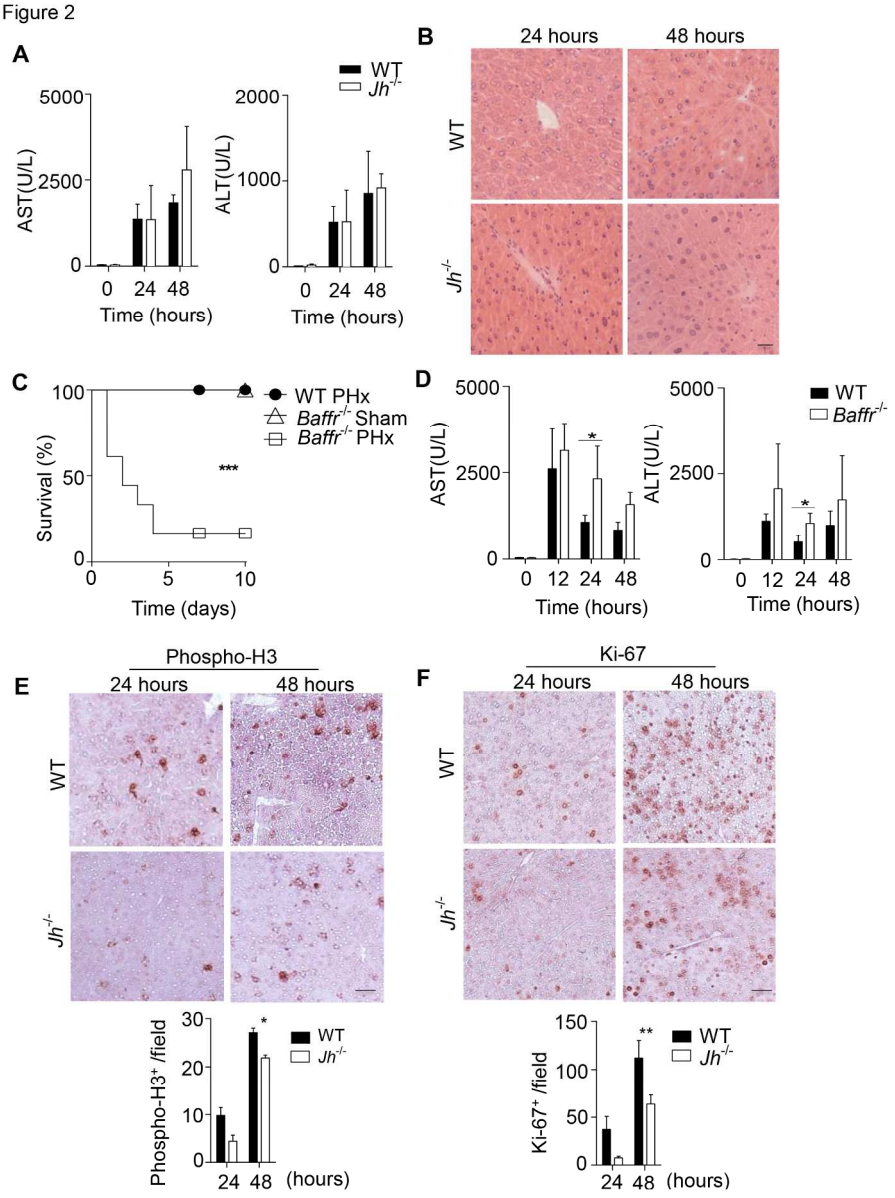

190x254mm (300 x 300 DPI)

Figure 3

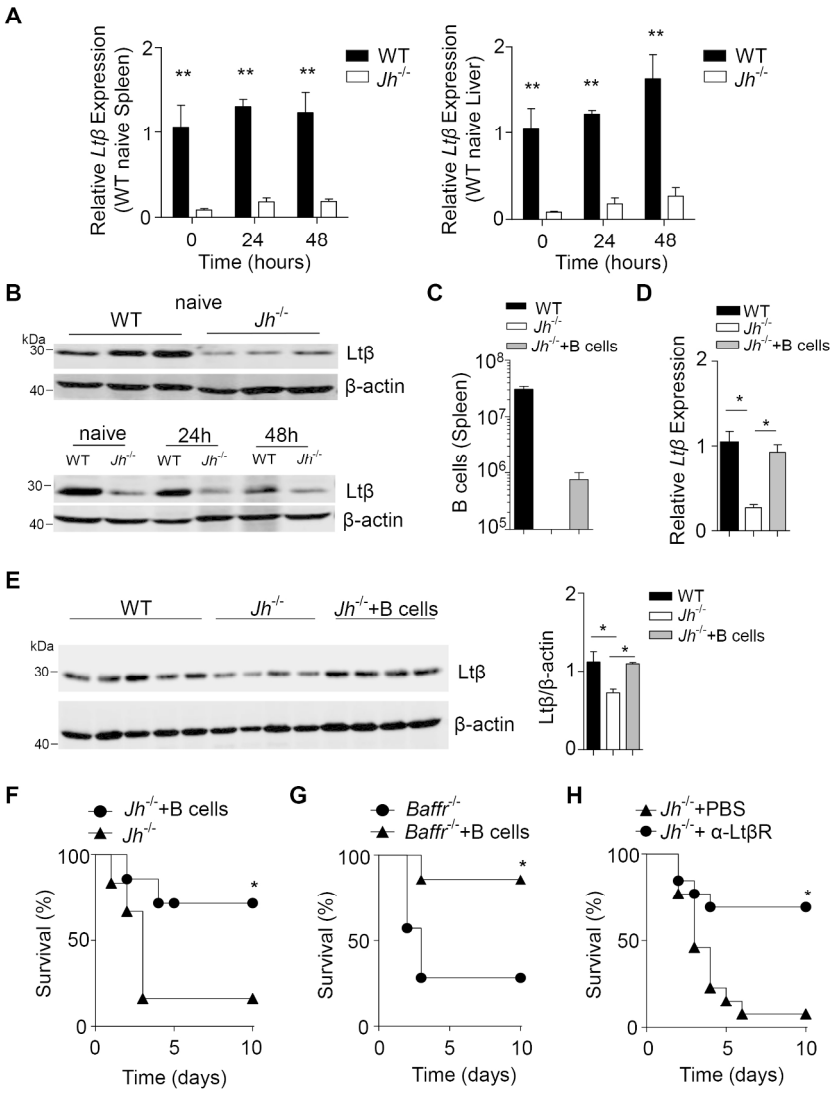

190x254mm (300 x 300 DPI)

Figure 5

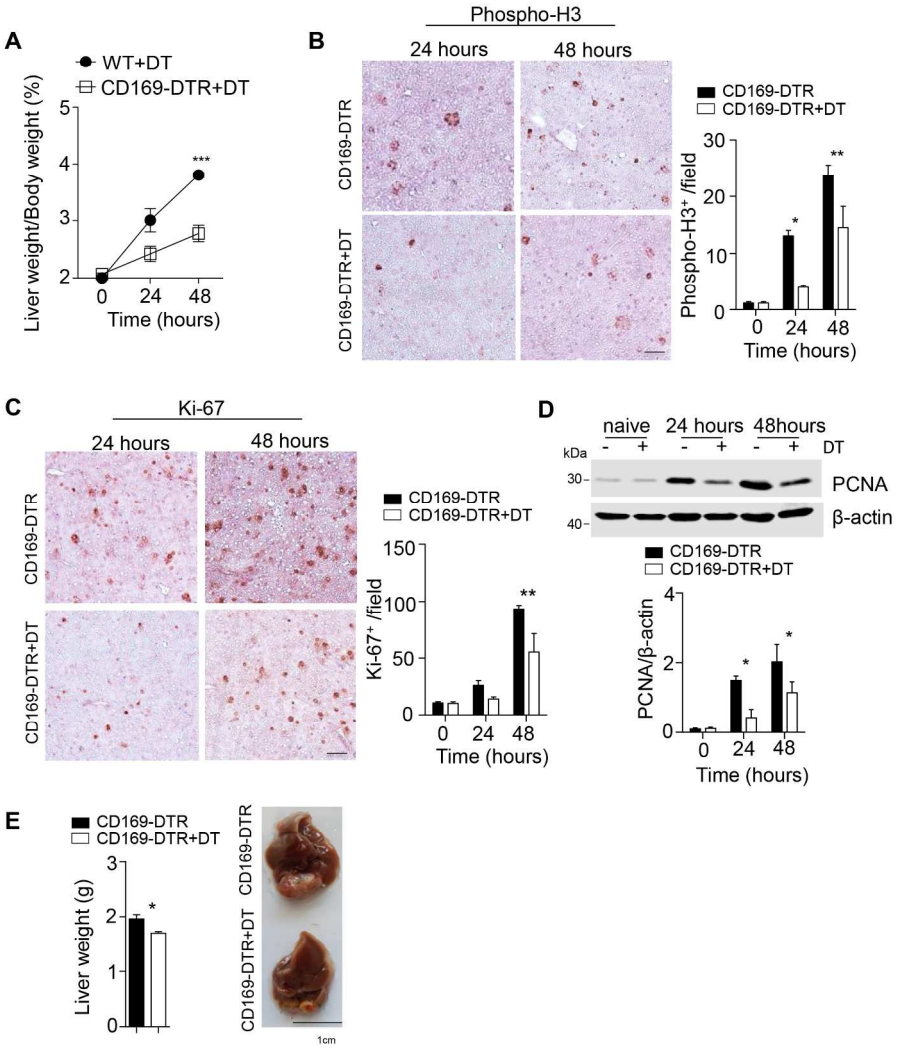

190x254mm (300 x 300 DPI)

Figure 6

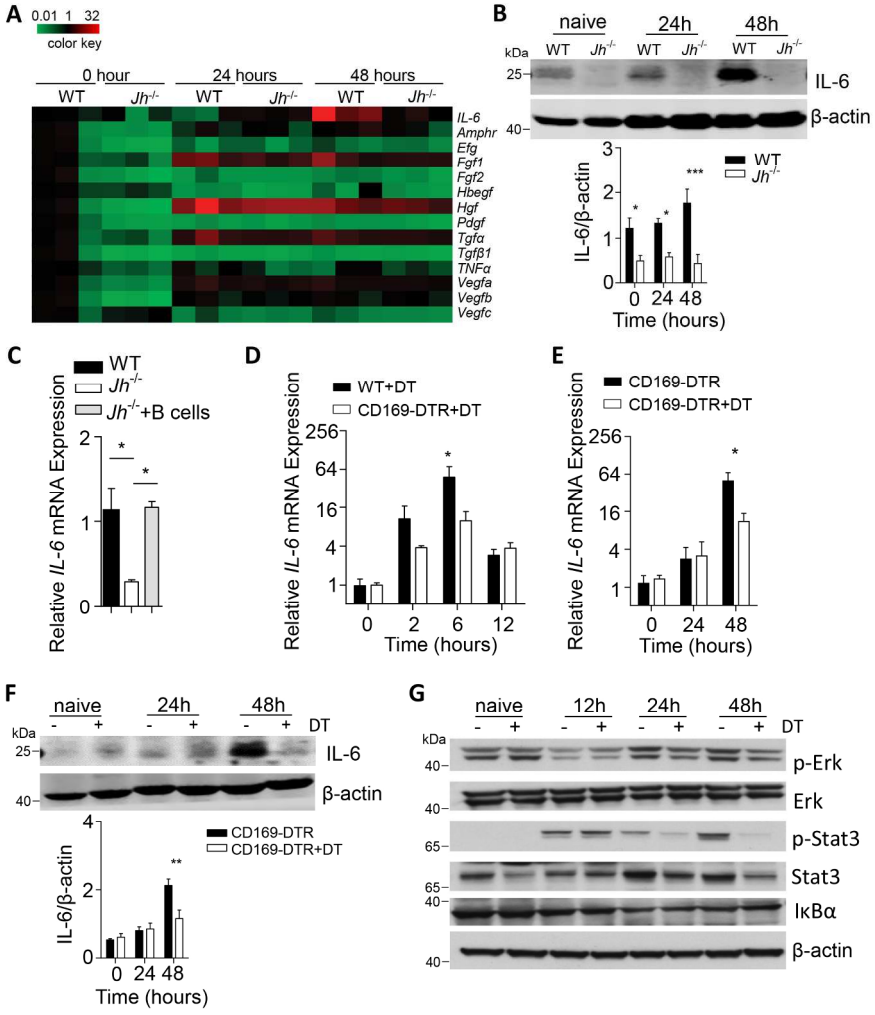

190x254mm (300 x 300 DPI)

Figure 7

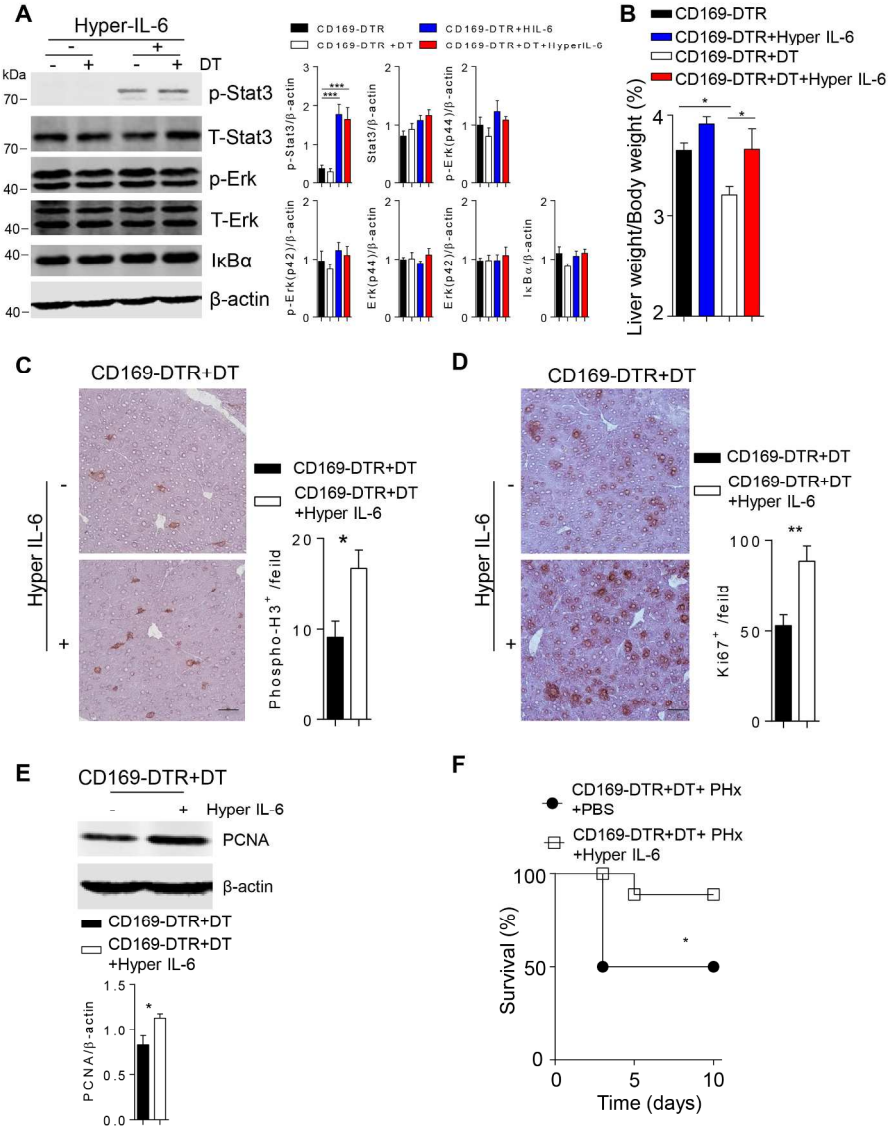

190x254mm (300 x 300 DPI)